

Ioan Ruja, Constantin Marta, Florin Brabăn

Research on the Command of a Single-Phase Frequency Converter at High Frequencies

The present paper forwards several results obtained during the study of the induction heating installations of metallic materials at high frequencies [1]. It details aspects related to the command of a mono-phase (half-bridge) inverter with PWM signals (Pulse-Width-Modulation). The command of the MOS transistors is done with frequencies ranging between $[0 \div 400]$ KHz and modulation factor variable within the $[0-1]$ range. The possibility to modify the command frequency of the inverter, as well as the possibility to modify the PWM signal modulation factor allows the user to establish various resonance frequencies for the LC (parallel) circuit which, together with the metallic sample, constitutes the inverter charge.

Keywords: heating, melting metallic, signal, induction, resonance

1. Introductory notions

1.1. The necessity of heating and melting metallic materials at high frequency.

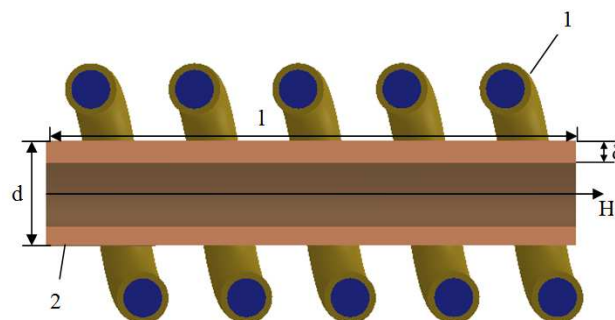


Figure 1. Detail regarding the induction heating of metals

- 1- inductor's coil
- 2- metal sample
- H- intensity of the magnetic field

The active electric power transmitted by the source of electric power to the full- cylinder-shaped metallic sample is:

$$P = K_0 \times d \times l \times H^2 \times \sqrt{\pi^3 \times \mu_0 \times \mu_r \times f \times \rho} \quad (1)$$

where:

K_0 - is an adaptation factor determined experimentally depending on the configuration of the inductor and the sample properties.

d - is the diameter of the metallic sample.

l - is the length of the sample.

μ_0 - void's absolute permeability

μ_r - relative permeability of the metallic material;

f - frequency of the feeding voltage

ρ - resistivity of the metallic material.

The dimension of the power transmitted to the sample in view of heating of melting may be realised as follows [2]:

- increasing the number of coil windings
- increasing the current through the inductor
- increasing the frequency of the supply frequency.

In order to rapidly growing the power transmitted to the metallic material, a source of electric power is required, by which one could easily increase the current through the inductor, the supply frequency or both [3].

In the case of exceeding the Curie point of the metallic sample, μ_r becomes 1, whereas the transmitted power decreases. It becomes thus useful to have the possibility of increasing the frequency, in order to compensate for the drop of μ_r .

The penetration depth of the magnetic field in the metal is:

$$\delta = 503 \sqrt{\frac{\rho}{\mu_r \cdot f}} \quad (2)$$

where :

δ - is the penetration depth [m]

f - is the frequency [Hz]

μ_r - is the relative energetic permeability;

ρ - is the resistivity [$\Omega \cdot m$]

1.2. Behaviour of metallic materials when treated with high frequencies.

The specialists' researches about the influence of frequency upon the physical and chemical properties of materials have determined the improvement of heating and melting technologies, as well the development of new equipment allowing the application of these technologies. Metals' hardening through induction at different frequencies is well known. In the case of melting, the frequency parameter influences: the thermal and electrical conductivity; magnetic permeability; toughness, resistance to tear; resistance to corrosion; plasticity; structure, homogeneity; ductility, tenacity, elasticity, forgeability, weldability. In the case of alloys, the influence of alloying elements (Mn, Si, P, S, Cr, Ni) refers to the modification of different metal properties, depending on the value of the frequency used [4].

We are witnessing an increasing interest for the metals melting in levitation (in electro-magnetic field), at high frequencies, with the purpose of obtaining purer materials, more homogenous and with specific structures [5].

The advantages of materials' heating and melting by induction, at high frequencies, are [6]:

- the possibility of reaching higher heating rates in air or void;
- the possibility of using higher power densities (kW/m^2);
- obtaining higher efficiencies of heating and melting installations with transistor frequency converters (75-90)% and the use of high frequency ranging between (0-500) KHz;
- obtaining high-purity materials;
- metal melting is optimum when one reaches the resonance frequency (f_r) which differs from one material to another depending on its chemical composition and dimensions;
- very favourable and environmentally friendly conditions and very low pollution.

1.3. Objectives of the study.

The research aimed at:

- commanding a mono-phase static frequency converter able to supply an output alternative voltage with variable frequency (0-400)KHz
- the possibility of modifying the filling factor of the PWM signal [7].

The study method was based on the drawing up of the electric diagram of generation and adaptation of PWM signals necessary for commanding the inverter, the simulation of the diagram operation and the comparison of experimental results with the simulated ones [8].

2. Considerations about the PWM signals

For the command of a mono-phase inverting half-bridge, with MOSFET transistors, we need two command channels with two PWM signals, phased as follows:

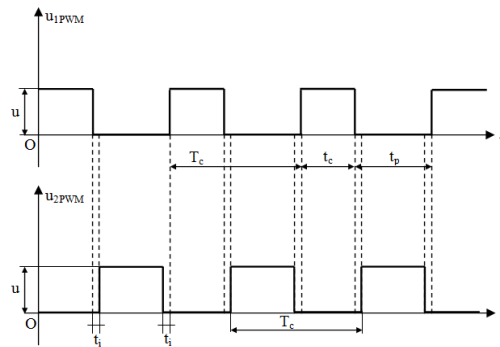


Figure 2. The wave shapes $u_{1PWM}^{(t)}$ and $u_{2PWM}^{(t)}$ for the half bridge command

Such signals ensure the rapid conduction input of MOS transistors as well as minimum conduction losses [9].

$$f_c = \frac{1}{T_c} \quad (3)$$

$$f_u = \frac{t_f}{t_f + t_p} = \frac{t_f}{T_c} \quad (4)$$

$$T_c = t_f + t_p \quad (5)$$

t_i – commutation delay

u – signal amplitude

f_c – command frequency

f_u – filling factor

T_c – period of the PWM signal

By the variation of the filling factor $f_u \in [0-1]$ we can modify the electric power transmitted to the inverter charge .

3. Considerations about the inverter.

The electric diagram of the inverter is shown in Figure 3. The command of the inverter is asymmetrical.

The inverter operates at a f_c commutation frequency, lower than the f_r resonance frequency of the $L_s C_s$ parallel oscillating circuit. The command frequency of

the inverter remains constant after having reached the resonance frequency of the $L_s C_s$ circuit [10].

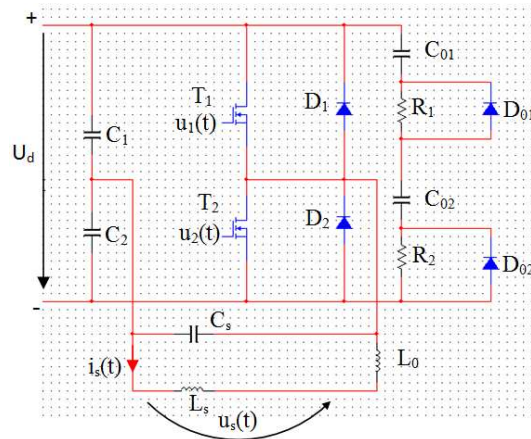


Figure 3. Electrical force diagram of the inverter

The wave shape of the voltage on the charge $u_s(t)$ is close to the sinusoid.

For the over-voltage protection of transistors snubbers are used.

L_0 is an inductance of ferrite core ensuring the adaptation of the inverter impedance to the $L_s C_s$ resonance circuit.

The working frequency of the inverter is: $f_c \in [0-400]$ KHz.

4. Experimental results

4.1. The electric command diagram is presented in Figure 4.

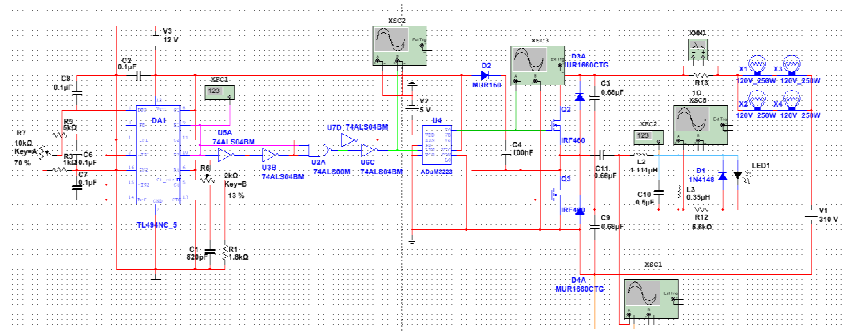
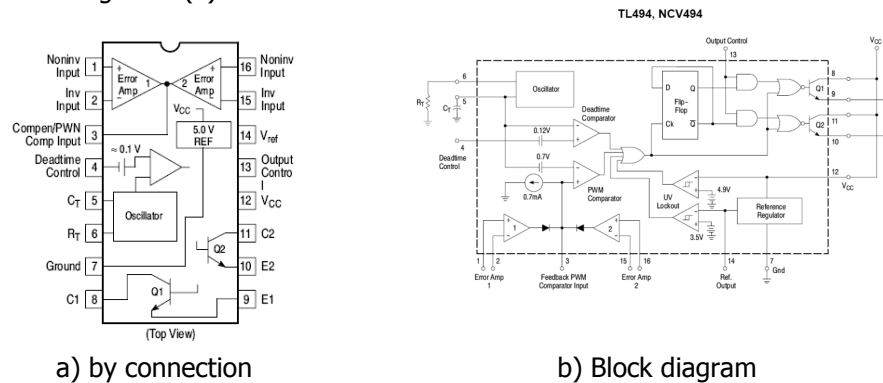


Figure 4. Electrical diagram of the frequency converter with $C_s L_s$ charge

4.2. The generator of PWM signals

The generation of PWM signals was done with the TL 494 integrated circuit presented in Figure 5 (a).



a) by connection b) Block diagram
Figure 5. Details of the TL494 integrated circuit

The galvanic separation of the command signals was done with the ADUM 3223 integrated circuit presented in Figure 6.

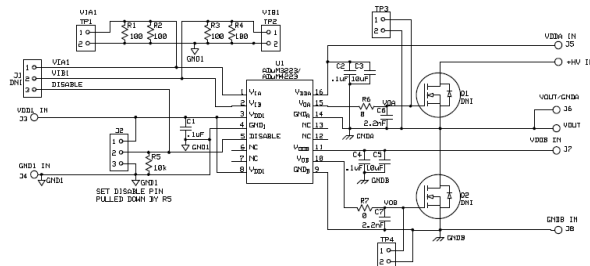


Figure 6. Details of the ADUM 3223 integrated circuit

4.3. The adaptation of the PWM signals to the parameters of the MOS transistors.

- the amplitude of the PWM signals is of 12 V, realised by the appropriate power supply of the ADUM 3223 integrated circuit
- the input current entering the source grid circuit of the transistor is of 6 A .
- the filling factor $f_u \in [0-1]$; the $f_u = 0,5$ was imposed
- the delay $t_i \cong 0$ s obtained through the passage of the U_2 PWM (t) signal through the chain of 74ALS04BM integrated circuits.

4.4. The shape of the PWM signals

Figure 7 presents the shape of the PWM signal, $u_{1PWM}(t)$ at the exit from the TL494 integrated circuit:

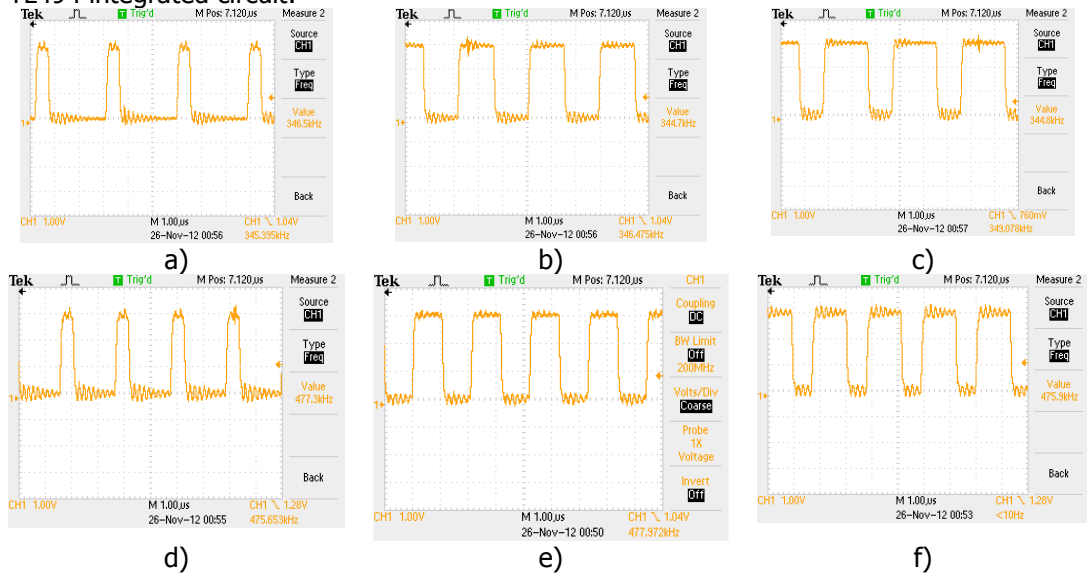


Figure 7. The wave shape of the $u_{1PWM}(t)$ signal at the exit from the TL494 circuit

where:

- a) $f_c = 345.39$ kHz and $f_u = 0.3$;
- b) $f_c = 346.47$ kHz and $f_u = 0.5$;
- c) $f_c = 349.07$ kHz and $f_u = 0.7$;
- d) $f_c = 475.65$ kHz and $f_u = 0.3$;
- e) $f_c = 477.97$ kHz and $f_u = 0.5$;
- f) $f_c = 475.9$ kHz and $f_u = 0.7$.

Figure 8 presents the wave shapes of the signals $u_{1PWM}(t)$ and delayed $u_{2PWM}(t)$.

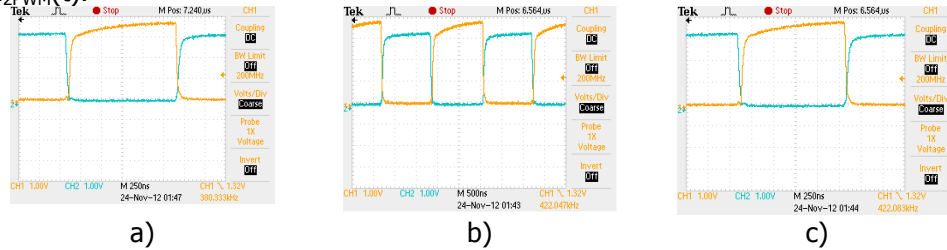


Figure 8. The wave shape of the $u_{1PWM}(t)$ signal and delayed $u_{2PWM}(t)$ signal

where:

- a) $f_c = 380.33 \text{ kHz}$ and $f_u = 0.5$;
- b) $f_c = 422.07 \text{ kHz}$ and $f_u = 0.5$;
- c) $f_c = 349.07 \text{ kHz}$ and $f_u = 0.5$ (zoom).

Figure 9 presents the wave shapes of the $u_{1PWM}(t)$ and $u_{2PWM}(t)$ signals on the grid of the MOS transistors:

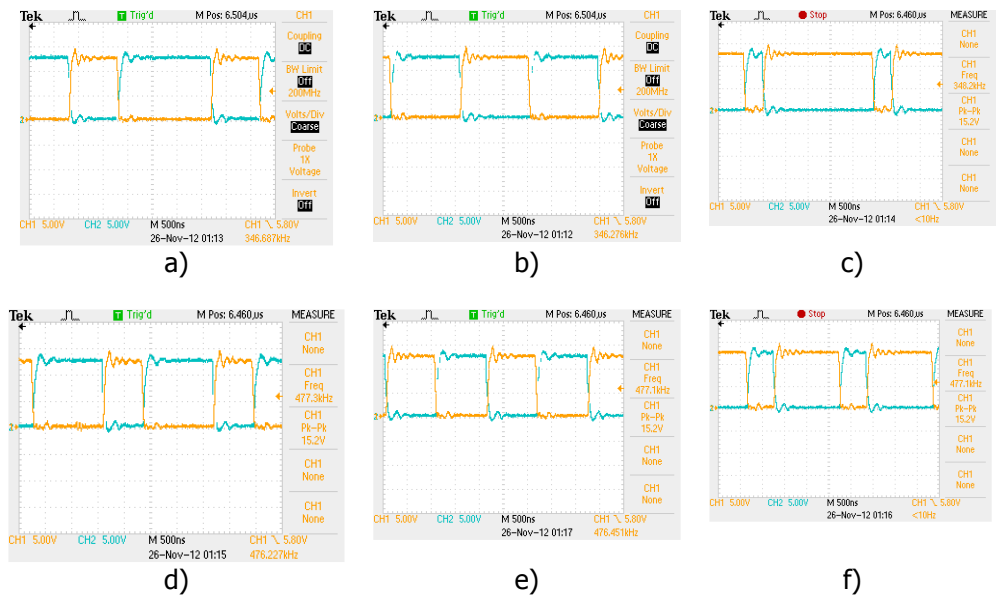


Figure 9. The wave shapes of the signals at $u_{1PWM}(t)$ and $u_{2PWM}(t)$ on the grid of the MOS transistors

where:

- a) $f_c = 346.68 \text{ kHz}$ and $f_u = 0.4$;
- b) $f_c = 346.27 \text{ kHz}$ and $f_u = 0.5$;
- c) $f_c = 348.02 \text{ kHz}$ and $f_u = 0.8$;
- d) $f_c = 476.22 \text{ kHz}$ and $f_u = 0.4$;
- e) $f_c = 476.45 \text{ kHz}$ and $f_u = 0.5$;
- f) $f_c = 477.1 \text{ kHz}$ and $f_u = 0.6$.

Figure 10 shows the wave shape of the $u_s(t)$ voltage at the charge entry with-out and with snubber circuits.

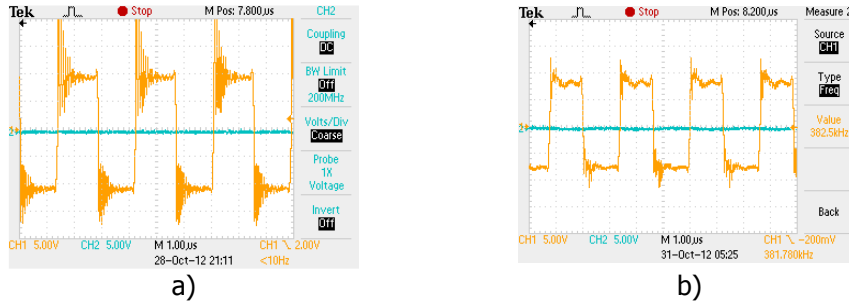


Figure 10. Wave shape of $u_s(t)$ voltage at the entry on the inverter charge

where:

- a) without snubber circuits at $f_c = 381.78 \text{ kHz}$;
- b) with snubber circuits at $f_c = 381.78 \text{ kHz}$.

Figure 11 presents in detail the 10 MHz-frequency parasite signals accompanying the PWM signals:

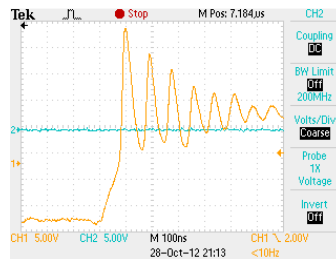


Figure 11. The 10 MHz-frequency parasite signal

Figure 12 presents in detail the commutation time at the command of the MOS transistors.

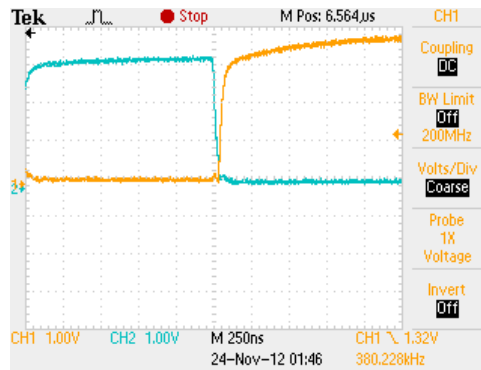


Figure 12. Delay, $t_i = 0s$, at $f_c = 380.22 \text{ kHz}$

5. Observations and conclusions

Following the experiments, the following conclusions could be drawn:

- The electrical diagram of delay and adaptation of PWM signals conceived and simulated by the authors was verified with good results in the inverter's operation.
- The delay obtained is approximately 0s , which leads to acceptable commutation losses;
- The maximum power transmission to the charge was obtained at a filling factor of $f_u=0.5$
- The command of transistors required a grid current with a peak of $I_{Gvf}= 6A$.
- The noise present in the composition of the PWM signals could not be eliminated, only reduced in amplitude and duration.
- The command driver for the MOSs should ensure a triggered signal so that the power dissipated on the transistors both in the ON and on the OFF state must be minimum; in order to achieve that, the increasing and decreasing fronts of the PWM signals should be as vertical as possible ($\frac{du}{dt} = (3,5 - 9)\frac{KV}{\mu s}$) whereas the higher and lower plateaux should not exhibit oscillations.
- The possible results obtained so far create the possibility of increasing the power of the static frequency converter as well as the command frequency, in order to diversify the types of materials subjected to the tests.

References

- [1] Zinn S., Semiatin S., *Elements of Induction Heating- Design Control and Application*, ASM International, 1988.
- [2] Dixon J., Tepper S., Moran L., *Practical evaluation of different modulation techniques for current- controlled voltage source inverters*, IEE Proc. Electr. Power Appl. Vol.143. No.4. July 1996.
- [3] Holtz J., *Pulse width Modulation for Electronic Power Conversion*, IEEE Proc. Vol.82. No.8. August 1994
- [4] Alexa D., Gatlan L., Ionescu F., Lazar A., *Power Converters with Resonant Circuits* (in original in Romanian), Technical Editions , Bucharest, Romania 1998
- [5] Bowes, S.R., Grewal S., *Three-level hysteresis band modulation strategy for single-phase PWM inverters*, IEE Proc. Electr. Power Appl. Vol.146. No. 6. Nov.1
- [6] Muntean, N., *Static Converters* (in original in Romanian), Polytechnic School Press, Timisoara, Romania, 1998.
- [7] Motorola; *TL494, Switchmode Puls Width Modulation Control Circuit*.

- [8] Analog Devices; *ADuM3223/ADuM4223, Isolated Precision Half-Bridge Driver.*
- [9] *Datasheetcatalog Power MOSFET; IXFN 100N50P.*
- [10] Bowes S.R., Lai Y.S., *Investigation into optimizing high switching frequency regular sampled PWM control for drives and static power converters,* IEE Proc.-Electr. Power Appl. Vol.143. No.4. July 1966.

Addresses:

- Prof. Dr. Eng. Ioan Ruja , "Eftimie Murgu" University of Reșița, Piața Traian Vuia, nr. 1-4, 320085, Reșița, i.ruja@uem.ro
- Conf. Dr. Eng. Constantin Marta, "Eftimie Murgu" University of Reșița, Piața Traian Vuia, nr. 1-4, 320085, Reșița, c.marta@uem.ro
- Prof. Dr. Florin Breabăn, Universite d'Artois, IUT Bethune, France, florin.breaban@univ-artois.fr